Far Field Reconstruction based on Compressive Sensing with Prior Knowledge

Baozhu Li [1], Wei Ke [*1,2], Huali Lu [1], Shuming Zhang [1], and Wanchun Tang [1,2]

[1] Jiangsu Province Engineerings Laboratory of Audio Technology
Nanjing Normal University, Nanjing, 210023, China
951408095@qq.com, kewei@njnu.edu.cn, 247588640@qq.com, 1627839409@qq.com, eewctang@njnu.edu.cn

[2] Jiangsu Center for Collaborative Innovation in Geographical Information Resource Development and Application
Nanjing, 210023, China

Abstract ─ Far field reconstruction in a large-scale space is time consuming and imprecise. However, if these data are sampled randomly and can be sparse on a specific transform domain, it will become quick and accurate to complete the field reconstruction by using the compressive sensing (CS). By taking the feature of the far field distribution for the half-wave dipole antenna in half space as an important prior knowledge, the sparse transform can be chosen appropriately. Moreover, a piece-wise approximation method is presented to reconstruct the far field. The simulated results show that this proposed method has better performance for far field reconstruction than the traditional method.

Index Terms ─ Field reconstruction, prior knowledge, sparse, compressive sensing.

I. INTRODUCTION

The spatial distribution of electromagnetic (EM) field [1] can provide an intuitive demonstration of radio wave propagation. Accordingly, estimating the totality of electromagnetic field existing at a given location precisely and rapidly offers guidance for wireless network optimization. Simulation softwares such as Wireless Insite [2] and Winprop [3] have been developed for the electromagnetic simulation. In fact, the results of these softwares are not accurate enough due to the complexity of the environment [4]. Therefore, field reconstruction based on measurement by monitoring a station or using a personal dosimeter is still needed. To describe the spatial distribution pattern of the electromagnetic radiation field in the entire region, an efficient method for field reconstruction is necessary [5].

Several interpolation methods can be used to perform EM field reconstruction. The model based parameter estimation (MBPE) [6-8] is used in computational electromagnetics based on polynomial fitting. In [9], a method of weighted minimization of two norms is proposed to interpolate the EM near field when no information on the radiating source is available. In [10], five spatial interpolation methods for electric field in urban environments are used and compared. However, these methods mentioned above do not perform very well in the large-scale geographic space due to the reflection, transmission and diffraction of EM waves. And in field reconstruction, no prior knowledge about EM field is used. Hence, it is necessary to develop new solutions to reconstruct the EM field.

In [11] the Bayesian compressive sensing algorithm is utilized to fast analyze the EM scattering problem. It is similar to the field reconstruction problem. Compressive sensing enables a signal to be reconstructed completely from a small set of nonadaptive, linear measurements by obtaining a sparse representation in some basis [12-14]. It has been applied to many EM problems [15-18]. Recently, it is used to reconstruct the complex time-harmonic electric field in [19]. The electric field is modeled as a summation of 20 incident homogeneous plane waves with random phase, magnitude, and angle-of-arrival. Actually, incidence, reflection, transmission, and diffraction are not independent of each other. The electric field in a real environment does not have such a sparse representation in the spatial-frequency domain. As an important prior knowledge, feature of EM wave propagation in real environment should be also considered for the field reconstruction.

Therefore, taking the electric field distribution created by a half-wavelength dipole antenna above the ground as an example, far field reconstruction in a large-scale space using compressive sensing is researched. Firstly, the prior knowledge about the electric field distribution feature is introduced. According to the prior knowledge, the selection of transforms for field reconstruction is discussed. Specifically, the method of piece-wise approximation reconstruction according to the prior knowledge is proposed. In the end, the electric field in a real environment is reconstructed by the

Submitted On: May 29, 2018
Accepted On: September 24, 2018

proposed method.

II. PRIOR KNOWLEDGE FOR FAR FIELD RECONSTRUCION

Various antennas exist in our lives. One of the most commonly used antenna is the half-wavelength dipole antenna. In this section, the feature of the electric field distribution for the half-wavelength dipole antenna in half space is analyzed. The feature will provide an important prior knowledge for the following field reconstruction.

A. Half-wavelength dipole antenna above the ground

Suppose the geographical space is divided into two half parts, the interface is a smooth plane. The upper half space is air and the lower half is ground. As a result, the total electric and magnetic field in the upper space with a certain height above the ground are the superposition of the incident and reflected components, as shown in Fig. 1.

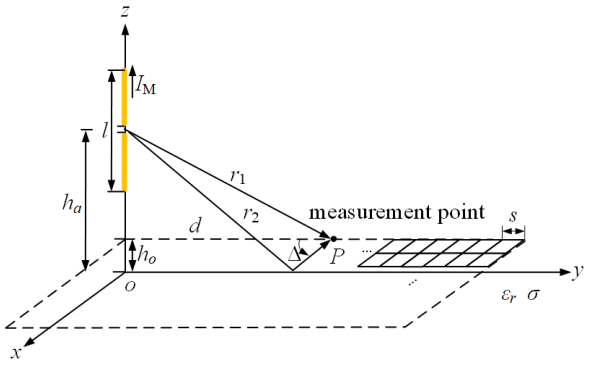

Fig. 1. A half-wavelength dipole antenna above the ground with the observation plane at height of h_o.

In Fig. 1, the observation plane is at a height of h_o above the ground and is divided into uniform grids with grid width of s. Due to the symmetry of the electric and magnetic field distribution on the observation plane, only the field distribution along the path d is studied. Other symbols in Fig. 1 are not described here for briefness.

Significantly, at the Brewster angle [20] of incidence, no TM wave is reflected for this vertical dipole antenna of Fig. 1. The Brewster angle can be calculated by:

$$\Delta_{r0} = \operatorname{arccot}\sqrt{\frac{\varepsilon_c}{\varepsilon_0}}, \tag{1}$$

where ε_c is the complex effective permittivity of ground. Thus, we have:

$$d_{r0} = \frac{h_a + h_o}{\tan\Delta_{r0}}. \tag{2}$$

That means, there is no reflection at $d=d_{r0}$, an important parameter for studying the feature of the electric field distribution.

B. The feature of the far field distribution as prior knowledge

In order to describe the feature of the far field distribution of the dipole antenna intuitively, one illustrative example of the calculation parameters shown in the Table 1 is given.

Table 1: Calculation parameters

Parameter	Value
s	1m
h_a	20m
h_o	2m
f	3GHz
I_M	1A
ε_r	25
σ	2×10^{-2}S/m

From Eqs. (1) and (2), one can obtain that d_{r0}= 110m. And the electric field distribution along the path d of Fig. 1 can be calculated and is shown in Fig. 2. All the measured points along this path d is in the far field region. The results show that the magnitude of the electric field increases with intense oscillation firstly and then decreases with slow oscillation when the observation point P moves away from the antenna.

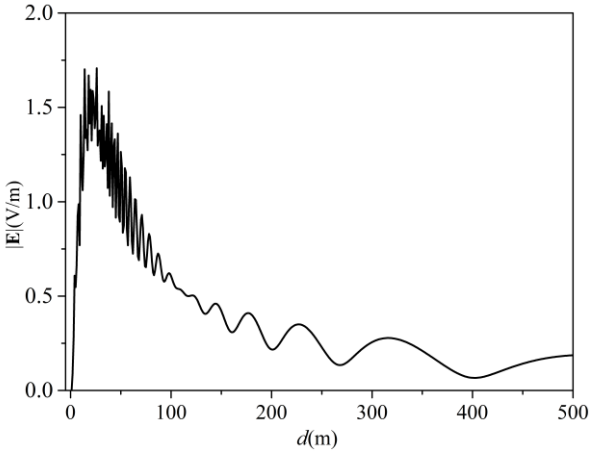

Fig. 2. Electric field distribution of the half-wavelength dipole antenna along the path d.

The feature of the electric field distribution is mainly caused by the phase differences of the incident and reflected waves. This can be explained as follows. When the measured point P is above the ground, there is a propagation path difference (r_1<r_2) between the incident wave and the reflected wave, as shown in Fig. 1. It leads to that the phase changes of the incident wave and the reflected wave are not synchronizable when P moves

away from the antenna. And if d is larger than d_{r0} and continues to increase, the propagation path difference between the incident and reflected waves becomes smaller and smaller, resulting that the phase difference between them oscillates more and more slowly.

Although only the electric field of the vertical dipole antenna above the ground is calculated, other types of antennas also have the above features. That is, when the observation plane is above the ground, the closer the measured point is to the antenna, the more intensely the electric field oscillates, and on the other hand the farther from the antenna, the more slowly the electric field oscillates. Therefore, the distance d_{r0} of Eq. (2) can be taken as an important prior knowledge for the field reconstruction.

III. ELECTRIC FIELD RECONSTRUCTION USING COMPRESSIVE SENSING

Electric field distribution of the antenna in space is not sparse in the measured domain. However it can be sparse on a specific transform domain. In this section the theory of field reconstruction based on compressive sensing with prior knowledge is studied.

A. Compressive sensing

Suppose that $\mathbf{x}$ is the original electric field to be reconstructed, it can be considered as a discrete signal with length of N. The signal $\mathbf{x}$ is compressible if there exists a basis matrix $\mathbf{\Psi}$ in that $\mathbf{x}$ becomes nearly sparse:

$$\mathbf{x}=\mathbf{\Psi\theta} \Leftrightarrow \mathbf{\theta}=\mathbf{\Psi}^{-1}\mathbf{x}\,, \tag{3}$$

where vector $\mathbf{\theta}$ is the representation of $\mathbf{x}$ in the domain of $\mathbf{\Psi}^{-1}$. If the number of non-zero coefficients in $\mathbf{\theta}$ is K ($K<<N$), it is called K-sparse signal.

The basis matrix $\mathbf{\Psi}$ is the inverse transform matrix, where the transform may be taken as one of the most popular orthogonal transforms: discrete Fourier transform (DFT), discrete cosine transform (DCT) and discrete wavelet transform (DWT). That is, $\mathbf{\Psi}$ transforms the sparse vector $\mathbf{\theta}$ into the original electric field $\mathbf{x}$ of interest.

On the other hand, the sampled vector $\mathbf{y}$ with $M\times1$ can be expressed as:

$$\mathbf{y}=\mathbf{\Phi x}=\mathbf{\Phi\Psi\theta}=\mathbf{A}^{CS}\mathbf{\theta}\,, \tag{4}$$

where $\mathbf{\Phi}$ is the measurement matrix with $M\times N$ ($M<N$) that is incoherent with $\mathbf{\Psi}$ and $\mathbf{A}^{CS}$ is the observation matrix. M is the number of measurements.

Here, one should note that the sampled vector $\mathbf{y}$ is actually sampled from the original electric field $\mathbf{x}$. Then $\mathbf{A}^{CS}$ can be converted to a partial random matrix by randomly selecting the rows of the matrix $\mathbf{\Psi}$.

$\mathbf{x}$ can be exactly reconstructed with overwhelming probability by (3). Under the conditions of $2K<M<N$ the reconstruction is equal to solve the l_0-norm optimization problem of Eq. (4), namely:

$$\min\left\|\mathbf{\theta}\right\|_0 \text{ s.t. } \mathbf{A}^{CS}\mathbf{\theta}=\mathbf{y}\,. \tag{5}$$

However, solving Eq. (5) is an non-deterministic polynomial-time hard problem. In order to reduce complexity, l_1-norm optimization problem is used as alternative, i.e.,

$$\min\left\|\mathbf{\theta}\right\|_1 \text{ s.t. } \mathbf{A}^{CS}\mathbf{\theta}=\mathbf{y}\,. \tag{6}$$

The reconstruction algorithm used in this paper is orthogonal matching pursuit (OMP) [21], which solves (6) by greedy iteration to approach the sampled vector $\mathbf{y}$.

B. Sparse representation

As described above, three most popular orthogonal transforms can be used. In this subsection, we will study how to select the transform from DFT, DCT and DWT appropriately according to the prior knowledge.

The reconstructed electric field in this paper is taken along the path d within the range of $1\text{m}\le d\le256\text{m}$, with N=256 sampled points. According to the prior knowledge of last section, this range can be divided into two parts at d=128m, that is, the region of $1\text{m}\le d\le128\text{m}$ with intense oscillation and the region of $129\text{m}\le d\le256\text{m}$ with slow oscillation.

In order to evaluate the sparsity of DFT, DCT, and DWT, we introduce another vector $\mathbf{\theta}$_normal as below:

$$\mathbf{\theta}\_\text{normal}=\frac{\mathbf{\theta}}{\left\|\mathbf{\theta}\right\|_2}\,. \tag{7}$$

By calculating the percentage of element in $\mathbf{\theta}$_normal less than a threshold ξ (taken as 0.005 in this paper), the sparsity comparison for the three transforms are shown in Table 2.

Table 2: The sparsity comparison of DFT, DCT, and DWT with ξ=0.005

Region	DCT	DWT	DFT
$1\text{m}\le d\le256\text{m}$	33.98%	71.48%	23.43%
$1\text{m}\le d\le128\text{m}$	23.19%	50.00%	7.81%
$129\text{m}\le d\le256\text{m}$	89.06%	82.81%	58.59%

Form Table 2, one can see that the sparsity percentage in region of $129\text{m}\le d\le256\text{m}$ can be up to 89.06% in DCT domain. In the region of $1\text{m}\le d\le128\text{m}$ and $1\text{m}\le d\le256\text{m}$, the sparsity percentage in DWT domain is the largest.

Furthermore, one can also find that DFT is not the optimal sparse basis transform in any region above. This is because the incident and reflected waves are not independent due to the ground reflection. Moreover, the plane wave angular spectrum varies with the change of propagation path. Therefore, the electric field is not very sparse in DFT domain.

From point view of signal and system, most of the signal energy is concentrated at the lower frequency after DCT, while DWT has more excellent multi-resolution properties than DCT. That means, for the reconstruction of the electric field, DCT is suitable in the region of

electric field with slower oscillation (the region of 129m≤d≤256m in Table 2), while DWT is suitable in the region of the electric field with intense oscillation (the region of 1m≤d≤128m in Table 2).

IV. NUMBERICAL RESULTS

If the electric field |**E**| is inherently 2-D, it can be expressed as the 1-D vector by stacking the matrix columns and is represented by **x** with a length of N. The sample **y** of the electric field **x** is performed by using a random measurement matrix **Φ** with dimension $M\times N$. Finally, field can be reconstructed by OMP. For each choice of **Φ**, the quality of the reconstruction is evaluated by computing the relative error between the original and reconstructed field as follows:

$$e=\frac{\left\|\mathbf{x}-\hat{\mathbf{x}}\right\|_2}{\left\|\mathbf{x}\right\|_2}, \tag{8}$$

where $\hat{\mathbf{x}}$ is the reconstructed field. By choosing, for example 1000, different measurement matrices **Φ**, the reconstruction error can be obtained by taking the average of the relative errors of Eq. (8).

A. Field reconstruction by traditional approach

The traditional approach to reconstruct the electric field is to sample in the entire interested region and reconstruct it using only one transform matrix. This subsection investigates and compares the reconstruction error versus the number of measurements M for the three different transforms. The reconstructed electric field is in the region of 1m≤d≤256m of Fig. 2.

Figure 3 illustrates the reconstruction error versus the number of measurements 10≤M≤250. It is observed that the quality of the reconstructed electric field is directly related to the sparsity of the three different transforms just as indicated in Table 2. When M >115, the quality of the reconstruction is the best by DWT.

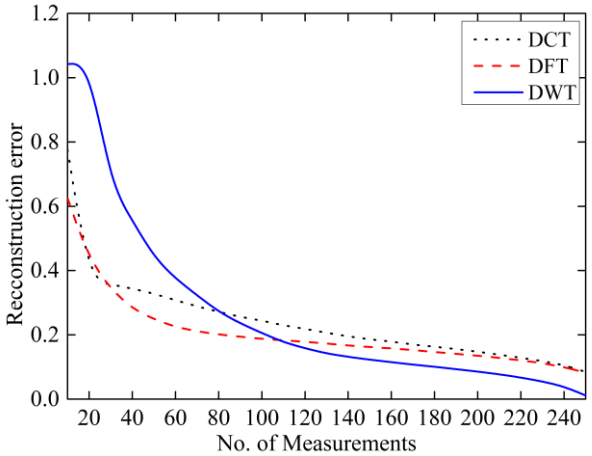

Fig. 3. Reconstruction error comparison in the region of 1m≤d≤256m for the three different transforms.

Next, we divide the region into two parts, including 1m≤d≤128m and 129m≤d≤256m, and reconstruct the electric field respectively. The results are shown in Fig. 4 and Fig. 5. As can be seen, in the region of 1m≤d≤128m, the reconstruction error by DWT is lower than DCT and DFT if M >55, while in the region of 129m≤d≤256m, the performance of DCT far exceeds that of the other two transforms.

It is also interesting to observe that the number of measurements M required for a good reconstruction depends on the complexity of the original electric field. As the distance from the source decreases, the oscillation of the field in the space becomes more and more intense, as a result, the more number of measurements are required to improve reconstruction.

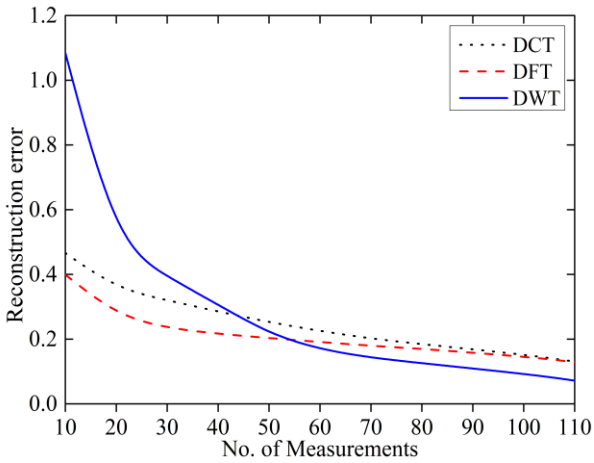

Fig. 4. Reconstruction error comparison in the region of 1m≤d≤128m for the three different transforms.

B. Field reconstruction by piece-wise approximation with prior knowledge

By dividing the whole region of 1m≤d≤256m into two parts according to d_{r0} by Eq. (2), a piece-wise approximation with prior knowledge is proposed. That is, DWT is used as the sparse transform with larger M in the region of 1m≤d≤128m, and instead, smaller M is required and DCT is adopted in the region of 129m≤d≤256m.

Figure 6 and Fig. 7 demonstrate the reconstructed electric fields in the region of 1m≤d≤256m (N=256) by traditional approach and the proposed approach, respectively. For the traditional approach, the reconstruction error is 0.201 with M=100 and using DWT. For the proposed approach, M is taken as 70 and 30 in the region of 1m≤d≤128m and 129m≤d≤256m, respectively. And the reconstruction error is 0.067.

Compared with the traditional approach, one can conclude that the piece-wise approximation with prior knowledge proposed in this paper needs less number of

measurements and has smaller reconstruction error.

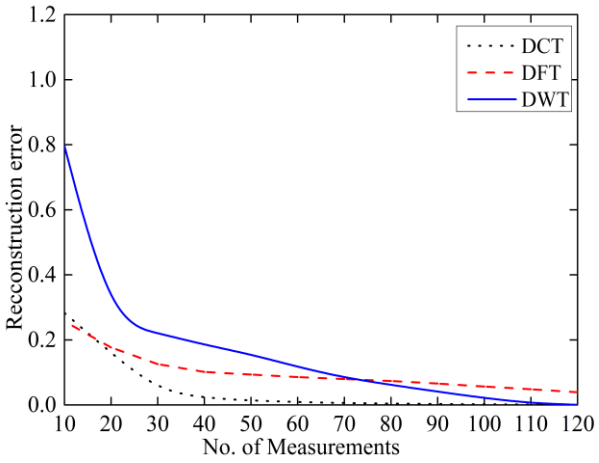

Fig. 5. Reconstruction error comparison in the region of 129m≤d≤256m for the three different transforms.

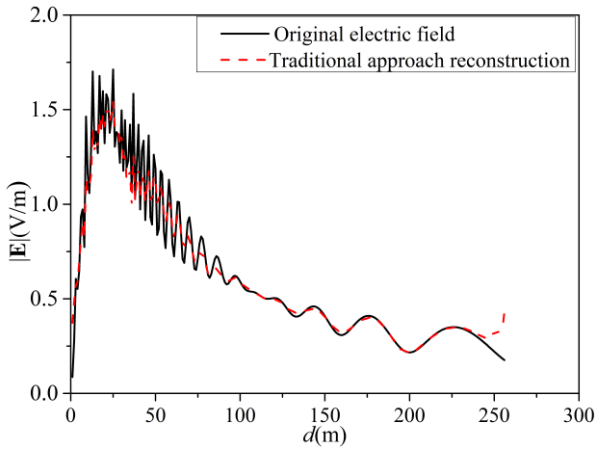

Fig. 6. Reconstructed electric field by the traditional approach and the original electric field.

C. Field reconstruction in real environment

In this subsection, the electric field in a real environment is reconstructed by compressive sensing. The original electric field is simulated in Wireless Insite [2]. There are 168×168 receivers (isotropic antenna) with spacing of 5m in a region of 840m×840m in this environment, as shown in Fig. 8. The transmitter (vertical half-wave dipole antenna) is located at the center of this region and the simulation parameters are listed in the Table 3.

Figure 9 shows the original electric field simulated by Wireless Insite. For field reconstruction, the total region is partitioned into 441 equal-sized cells with the area of 40m×40m.

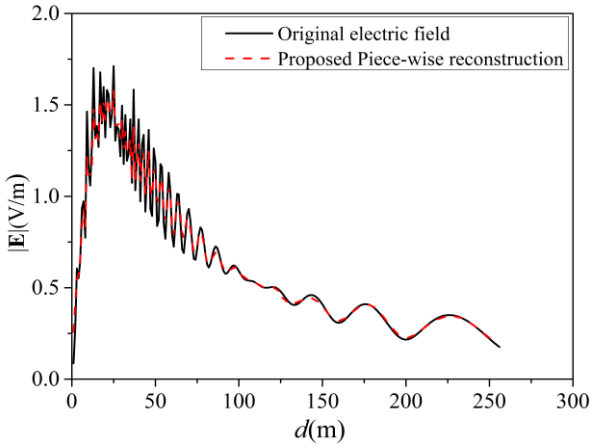

Fig. 7. Reconstructed electric field by the proposed approach and the original electric field.

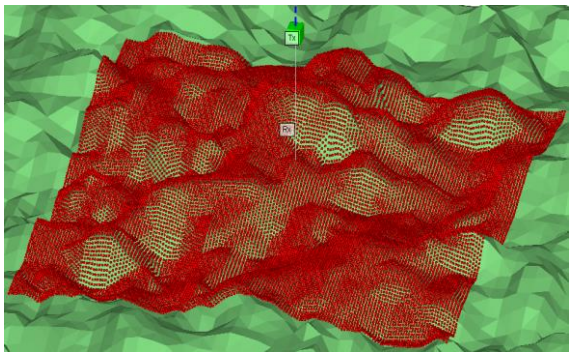

Fig. 8. A real environment modeled in Wireless Insite.

Table 3: Simulation parameters

Parameter	Value
s	5m
h_a	50m
h_o	2m
f	3GHz
I_M	1A
ε_r	25
σ	2×10^{-2}S/m

For the traditional approach with DWT, 20% of the number of measurements in each cell are used. The reconstructed electric field is shown in Fig. 10, with the reconstruction error of 0.7308.

For the proposed piece-wise approximation approach, d_{r0} is 260m by Eq. (2). Hence, a squire boundary with the side length of 520m divides the whole region of 840m×840m into two parts, as depicted in Fig. 9. Inside the boundary, DWT is used with 40% measurements, while outside the boundary, DCT is adopted with 20% measurements. The reconstructed

electric field is shown in Fig. 11 with the reconstruction error of 0.1972. Compared with the traditional approach, the proposed piece-wise approximation approach has better performance with not too more measurements increased.

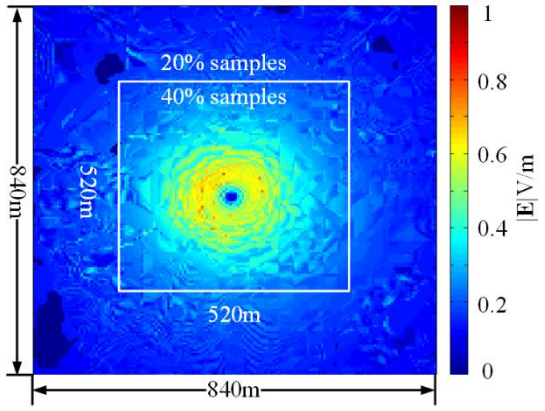

Fig. 9. Original electric field and the number of measurements.

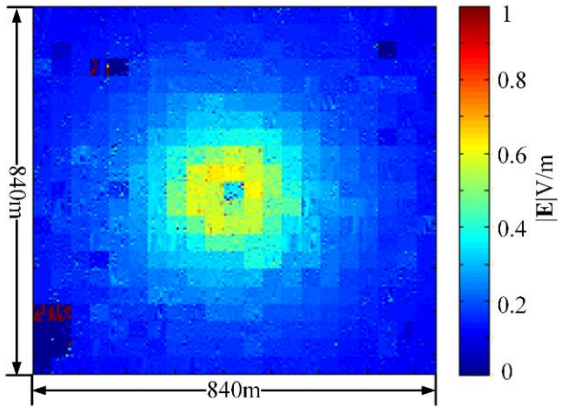

Fig. 10. Reconstructed electric field by the traditional approach.

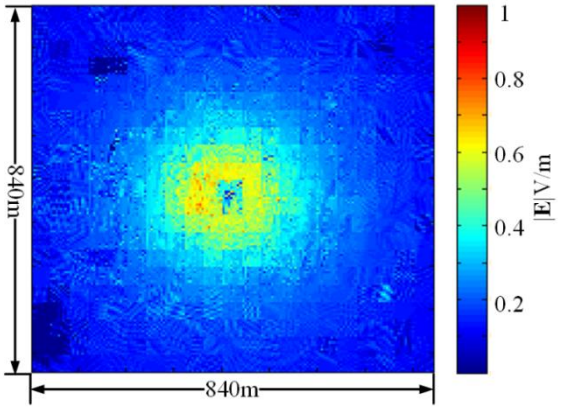

Fig. 11. Reconstructed electric field by the proposed approach.

V. CONCLUSION

The far field feature of half-wave dipole antenna in large-scale half-space is studied and taken as a prior knowledge for the electric field reconstruction by compressive sensing. With this prior knowledge, a new method based on the piece-wise approximation reconstruction is presented. Compared with the traditional approach, the proposed piece-wise approximation method can obtain a higher quality reconstruction field with an appropriate number of measurement points. In the end, the reconstruction in a real environment illustrates the validity and feasibility of the proposed method.

ACKNOWLEDGMENT

This work is supported by the National Key Research and Development Program of China (Grant No. 2017YFB0503500) and the National Natural Science Foundation of China (Grant No. 61571232).

The authors would like to thank Prof. Andrew Massa and Prof. Marco Donald Migliore in the research center of ELEDIA, Italy, for their theoretical guidance on this paper.

REFERENCES

[1] M. Salovarda and K. Malaric, "Measurements of electromagnetic smog," *IEEE Electrotechnical Conference*, Malaga, Spain, pp. 470-473, July 2006.

[2] P. Mededovic, M. Veletic, and Z. Blagojevic, "Wireless insite software verification via analysis and comparison of simulation and measurement results," *Mipro, 2012 Proceedings of the, International Convention IEEE*, Opatija, Croatia, pp. 776-781, July 2012.

[3] R. Hoppe, G. Wölfle, and U. Jakobus, "Wave propagation and radio network planning software WinProp added to the electromagnetic solver package FEKO," *Applied Computational Electromagnetics Society Symposium*, Florence, Italy, pp. 1-2, Mar. 2017.

[4] Y. O. Isselmou, H. Wackernagel, W. Tabbar, et al., "Geostatistical interpolation for mapping radio-electric exposure levels," *IEEE Conference on Antennas and Propagation*, Nice, France, pp. 1-6, Nov. 2006.

[5] C. C. Rodríguez, C. A. Forero, and H. O. Boada, "Electromagnetic field measurement method to generate radiation map," *IEEE Communications Conference*, Cali, Colombia, pp. 1-7, July 2012.

[6] E. K. Miller, "Model-based parameter estimation in electromagnetic Pt. 1," *IEEE Antennas and Propagation Magazine*, vol. 40, no. 1, pp. 40-52, Feb. 1998.

[7] E. K. Miller, "Model-based parameter estimation in electromagnetic Pt. 2," *IEEE Antennas and Propagation Magazine*, vol. 40, no. 2, pp. 51-65,

Apr. 1998.
[8] E. K. Miller, "Model-based parameter estimation in electromagnetic Pt. 3," *IEEE Antennas and Propagation Magazine*, vol. 40, no. 3, pp. 49-66, June 1998.
[9] B. Fuchs, L. L. Coq, and M. D. Migliore, "On the interpolation of electromagnetic near field without prior knowledge of the radiating source," *IEEE Trans. Antennas Propagat*., vol. 65, no. 7, pp. 568-3574, May 2017.
[10] T. A. A. Santana, H. D. D. Andrade, I. S. Q. Júnior, et al., "Comparison of spatial interpolation methods to determine exposure ratio to electric field in urban environments," *Electronics Letters*, vol. 53, no. 18, pp. 1250-1252, Sep. 2017.
[11] H. H. Zhang, W. E. I. Sha, and L. J. Jiang, "Fast monostatic scattering analysis based on Bayesian compressive sensing," *International Applied Computational Electromagnetics Society Symposium*, Florence, Italy, pp. 1-2, Mar. 2017.
[12] E. J. Candès, J. Romberg, and T. Tao, "Terence. robust uncertainty principles: Exact signal reconstruction from highly incomplete frequency information," *IEEE Trans. on Infor. Theory*, vol. 52, no. 2, pp. 489-509, Jan. 2006.
[13] D. L. Donoho, "Compressed sensing," *IEEE Trans. on Infor. Theory*, vol. 52, no. 4, pp. 1289-1306, Apr. 2006.
[14] E. J. Candès and T. Tao, "Near-optimal signal recovery from random projections: Universal encoding strategies?," *IEEE Trans. on Infor. Theory*, vol. 52, no. 12, pp. 5406-5425, Nov. 2006.
[15] B. Verdin and P. Debroux, "2D and 3D far-field radiation patterns reconstruction based on compressive sensing," *Progress in Electromagnetic Research M*, vol. 46, pp. 47-56, 2006.
[16] B. Verdin and P. Debroux, "Reconstruction of missing sections of radiation patterns using compressive sensing," *IEEE International Symposium on Antennas and Propagation & Usnc/ursi National Radio Science Meeting*, Vancouver, Canada, pp. 780-781, Oct. 2015.
[17] A. Massa, P. Rocca, and G. Oliveri, "Compressive sensing in electromagnetics-A review," *IEEE Trans. Antennas Propagat*., vol. 57, no. 1, pp. 224-238, Feb. 2015.
[18] G. Oliveri, M. Salucci, N. Anselmi, and A. Massa, "Compressive sensing as applied to inverse problems for imaging: Theory, applications, current trends, and open challenges," *IEEE Trans. Antennas Propagat*., vol. 59, no. 5, pp. 34-46, Aug. 2017.
[19] A. C. M. Austin and M. J. Neve, "Efficient field reconstruction using compressive sensing," *IEEE Trans. Antennas Propagat*., vol. 66, no. 3, pp. 1624-1627, Jan. 2018.
[20] J. A. Kong, *Electromagnetic Wave Theory*. John Wiley & Sons, Canada, 1985.
[21] J. Tropp and A. Gilbert, "Signal recovery from partial information via orthogonal matching pursuit," om highly incomplete frequency information," *IEEE Trans. on Infor. Theory*, vol. 53, no. 12, pp. 4655-4666, Apr. 2005.

Baozhu Li was born in Henan Province, China, in 1990. She received the B.S. degree from Nanjing Normal University Zhongbei College, Nanjing, in Electrical Engineering in 2013. She is working towards the Ph.D. degree with the School of Physics and Technology, NJNU. Her research interests include electromagnetic environment, antennas and signal processing.

Wei Ke received his M.S. degree in Communication Engineering from Nanjing Norm University, China, in 2002, and Ph.D. degree in Signal and Information Processing from Southeast University, China, in 2011. Since 2013, he has been an Associate Professor in Nanjing Norm University, China. His current main research interest is wireless positioning techniques.